

Bis(4-cyano-1-pyridino)pentane halobismuthates. Light-harvesting material with an optical band gap of 1.59 eV

Vitalii Yu. Kotov,^{*a,b} Andrey B. Ilyukhin,^a Alexey A. Sadovnikov,^a Kirill P. Birin,^c
Nikolai P. Simonenko,^a Hang Thi Nguyen,^a Alexander E. Baranchikov^{a,d} and Sergey A. Kozyukhin^a

^a N. S. Kurnakov Institute of General and Inorganic Chemistry, Russian Academy of Sciences, 117907 Moscow, Russian Federation. E-mail: VYuKotov@gmail.com

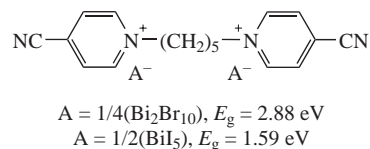
^b Higher Chemical College, Russian Academy of Sciences, 125047 Moscow, Russian Federation

^c A. N. Frumkin Institute of Physical Chemistry and Electrochemistry, Russian Academy of Sciences, 119071 Moscow, Russian Federation

^d Department of Chemistry, M. V. Lomonosov Moscow State University, 119991 Moscow, Russian Federation

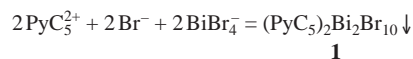
DOI: 10.1016/j.mencom.2017.05.018

A new organic-inorganic hybrid material composed of 0-D bromobismuthate anions and bis(4-cyano-1-pyridino)pentane cations was synthesized and characterized. The replacement of Br with I resulted in a decrease in the optical band gap from 2.88 eV for $(C_{17}H_{18}N_4)_2Bi_2Br_{10}$ to 1.59 eV for $(C_{17}H_{18}N_4)BiI_5$. Thus, $(C_{17}H_{18}N_4)BiI_5$ can be proposed as a candidate material for solid state solar cells.



Solar light is one of the most attractive energy sources;¹ its conversion into electricity is performed in photovoltaic devices.^{2,3} The most efficient solar cells are based on silicon or GaAs; however, a search for new inexpensive light-harvesting materials is of considerable current interest. The use of solid state solar cells, whose efficiency has been demonstrated for hybrid haloplumbate based cells,^{1,4} is promising. The main problems of light-harvesting perovskite materials are the presence of toxic lead and the poor stability of MAPbI₃, especially in moist air. Therefore, it is important to obtain nontoxic semiconductor materials which absorb solar light.^{5–10} Recently, it was shown that the hybrid halobismuthate materials based on bis(4-cyano-1-pyridino)propane or bis(4-cyano-1-pyridino)butane possess interesting properties. In particular, their optical band gaps (E_g) are as small as 1.70 and 1.76 eV, respectively.¹¹

Bis(4-cyano-1-pyridino)pentane bromide $C_{17}H_{18}N_4Br_2$ (PyC_5Br_2) was synthesized from 4-pyridinecarbonitrile and 1,5-dibromopentane.¹² The interaction of bis(4-cyano-1-pyridino)pentane cations with bromobismuthate anions (produced from the reaction between bismuth nitrate and excess potassium bromide) rapidly occurs in aqueous solution with the formation of a milky white product:



Compound **1**[†] is moderately soluble in DMF, DMSO or boiling water giving light yellow (DMF or DMSO) or colorless (boiling water) solutions. The crystals of **1** (Figure 1)[‡] were obtained by recrystallization from a saturated aqueous KBr

[†] According to the DTG results, compound **1** is anhydrous, mp 251 °C (decomp.). ¹H NMR (600 MHz, DMSO-*d*₆) δ: 9.46 (d, 4H), 8.76 (d, 4H), 4.73 (t, 4H), 2.02 (m, 4H), 1.36 (p, 2H). The atomic ratios according to EDX (Figure S5): Bi/(Br+I) = 1 : 5.1, Br/I = 5.1 : 0.0.

solution. X-ray powder diffraction (XRD) analysis was used to control the crystalline phase purity (Figure S7, see Online Supplementary Materials).

The interaction of bis(4-cyano-1-pyridino)pentane cations and iodobismuthate anions (resulted from the reaction between

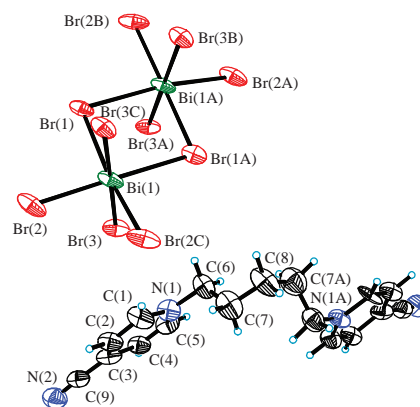
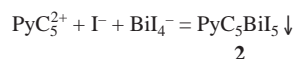


Figure 1 Structure fragment of **1**.

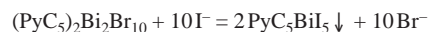
[‡] Calculations were fulfilled with the SHELXS-2014 and SHELXL-2014 programs.¹⁵ Experimental intensities were measured on a Bruker SMART APEX II diffractometer (graphite monochromated MoK α radiation, $\lambda = 0.71073 \text{ \AA}$) using ω -scan mode. The structures were solved by direct methods and refined by full matrix least squares on F^2 with anisotropic thermal parameters for all non-hydrogen atoms.

Crystal data for **1**. White block (0.10 × 0.04 × 0.02 mm), orthorhombic, space group $Fddd$, at 150 K: $a = 11.732(3)$, $b = 24.082(7)$ and $c = 33.431(9) \text{ \AA}$, $V = 9445(4) \text{ \AA}^3$, $Z = 8$, $d_{\text{calc}} = 2.495 \text{ g cm}^{-3}$. Total of 9499 reflections were collected ($2.4^\circ < \theta < 26.8^\circ$), $\mu = 15.938 \text{ mm}^{-1}$, 2501 independent reflections ($R_{\text{int}} = 0.1670$) and 1591 with $I > 2\sigma(I)$. Data/restraints/parameters: 2501/6/124. The final refinement parameters were: $R_1 = 0.0692$, $wR_2 = 0.2019$ for reflections with $I > 2\sigma(I)$; $R_1 = 0.1163$, $wR_2 = 0.2303$ for all reflections; largest diff. peak/hole 2.553, $-2.876 \text{ e \AA}^{-3}$. GOF = 1.187.

bismuth nitrate and excess potassium iodide) in aqueous solution led to black iodobismuthate **2**.[§]



This product can also be obtained by the interaction of **1** with potassium iodide in aqueous solution:



According to the XRD data (see Figure S4), product **2** is not an individual salt. Similarly, we observed the formation of a mixture of iodobismuthates in the reaction of bis(4-methyl-1-pyridino)pentane (PiC_5^{2+}) bromide with iodobismuthate acid. In accordance with single crystal XRD data, the main reaction product of the picoline derivative is black PiC_5BiI_5 with a 1-D anion structure, and red $(\text{PiC}_5)_2\text{Bi}_4\text{I}_{16}$ with a 0-D anion structure is a by-product. Thus, on the basis of the NMR (Figure S2) and EDX data (Figure S6), we presume that **2** is a mixture of different bis(4-cyano-1-pyridino)pentane iodobismuthates with black PyC_5BiI_5 as the main reaction product. This fine mixture cannot be separated mechanically unlike a mixture of products obtained in the reaction of bis(4-methyl-1-pyridino)pentane bromide and iodobismuthate acid.

The black precipitate of **2** is soluble in DMF or DMSO and moderately soluble in acetonitrile or boiling water. Our attempts to crystallize a black compound from DMF or acetonitrile were

All five checked single crystals of **1** were aggregates, the best of them containing at least four domains. We failed to split the array using the Cell_Now program;¹⁶ thus, the accuracy of the structure determination is low. The structure of **1** was refined by the Rietveld method using the TOPAS program.¹⁷ Details of the refinement for **1**: space group $Fddd$, at 296 K: $a = 11.7775(2)$, $b = 24.5073(9)$ and $c = 33.7288(12)$ Å; $R_{\text{exp}} = 2.49\%$, $R_{\text{wp}} = 6.97\%$, $R_p = 4.69\%$, and GOF = 2.80.

Crystal data for 3. Dark red needle ($0.24 \times 0.08 \times 0.06$ mm), monoclinic, space group $C2/c$, at 150 K: $a = 16.7446(10)$, $b = 12.8796(8)$ and $c = 12.9113(8)$ Å, $\beta = 100.799(2)^\circ$, $V = 2735.2(3)$ Å³, $Z = 4$, $d_{\text{calc}} = 2.525$ g cm⁻³. Total of 18095 reflections were collected ($2.4^\circ < \theta < 30.5^\circ$), $\mu = 6.824$ mm⁻¹, 4141 independent reflections ($R_{\text{int}} = 0.0549$) and 2710 with $I > 2\sigma(I)$. Data/restraints/parameters: 4141/0/123. The final refinement parameters were: $R_1 = 0.0341$, $wR_2 = 0.0555$ for reflections with $I > 2\sigma(I)$; $R_1 = 0.0719$, $wR_2 = 0.0649$ for all reflections; largest diff. peak/hole 0.696, -0.791 eÅ⁻³. GOF = 0.988.

Crystal data for 4. Red-orange needle ($0.28 \times 0.10 \times 0.08$ mm), orthorhombic, space group $Pbcn$, at 150 K: $a = 11.2492(4)$, $b = 20.1404(8)$ and $c = 14.0166(5)$ Å, $V = 3175.6(2)$ Å³, $Z = 4$, $d_{\text{calc}} = 2.765$ g cm⁻³. Total of 37376 reflections were collected ($2.5^\circ < \theta < 30.5^\circ$), $\mu = 11.412$ mm⁻¹, 4841 independent reflections ($R_{\text{int}} = 0.0548$) and 3911 with $I > 2\sigma(I)$. Data/restraints/parameters: 4841/0/146. The final refinement parameters were: $R_1 = 0.0271$, $wR_2 = 0.0595$ for reflections with $I > 2\sigma(I)$; $R_1 = 0.0399$, $wR_2 = 0.0640$ for all reflections; largest diff. peak/hole 1.612, -1.041 eÅ⁻³. GOF = 0.990.

The refinements were carried out using the TOPAS program.¹⁷ Details of the Rietveld refinement for **4** (product or recrystallization of **2** from 5.6 M KI solution under hydrothermal conditions): space group $Pbcn$, at 296 K: $a = 11.244(8)$, $b = 20.074(14)$ and $c = 14.103(9)$ Å; $R_{\text{exp}} = 4.64\%$, $R_{\text{wp}} = 5.95\%$, $R_p = 4.54\%$, GOF = 1.28.

CCDC 1511790–1511792 contain the supplementary crystallographic data for this paper. These data can be obtained free of charge from The Cambridge Crystallographic Data Centre via <http://www.ccdc.cam.ac.uk>.
[§] According to the DTG results, product **2** is anhydrous, mp 270 °C (decomp.). ¹H NMR (600 MHz, DMSO-*d*₆) δ : 9.39 (d, 4H), 8.76 (d, 4H), 4.68 (t, 4H), 2.00 (m, 4H), 1.34 (p, 2H). Ratio Bi/(Br+I) (EDX) = 1.0:4.9. Ratio Br/I (EDX) = 0.2:4.7. According to EDX mapping the presence of Br in the sample related to the formation of **1** as an impurity [ratio Bi/(Br+I) (EDX) = 1.00:4.93, ratio Br/I (EDX) = 4.74:0.19]. For areas where inclusions of the microcrystals of **1** are not observed, the atomic ratios are the following: Bi/(Br+I) (EDX) = 1.00:4.95, Br/I (EDX) = 0.03:4.92.

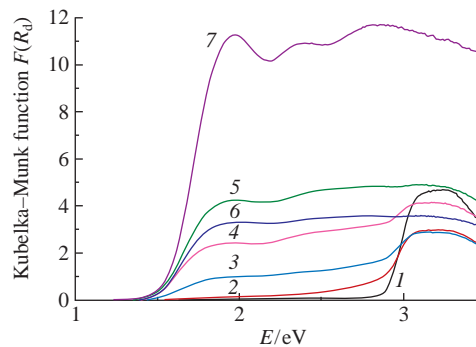


Figure 2 Diffuse reflectance spectra of samples (1) **1**, (2) **2a**, (3) **2b**, (4) **2c**, (5) **2d**, (6) **2e** and (7) **2**.

unsuccessful. The recrystallization of **2** from aqueous solution in air resulted in the formation of thin dark red needles[‡] of bis(4-cyano-1-pyridino)pentane triiodide, $\text{C}_{17}\text{H}_{18}\text{N}_4\text{I}_6$ [$\text{PyC}_5(\text{I}_3)_2$] **3**. Bis(4-amido-1-pyridino)pentane dihydronium iodobismuthate dihydrate, $\text{C}_{17}\text{H}_{27}\text{N}_4\text{O}_4\text{BiI}_6$ **4** was isolated as orange-red crystals[‡] during the recrystallization of **2** from concentrated HI or 5.6 M aqueous solution of KI under hydrothermal conditions (120 °C, 24 h). The heating of compound **4** leads to the loss of two water molecules at 120–160 °C, two water molecules at 160–230 °C, and an HCN molecule at 230–257 °C. Therefore, the composition of the thermolysis product differs from that of **2** and thermolysis cannot be used for its preparation.

The diffuse reflectance spectra of bis(4-cyano-1-pyridino)propane halobismuthates are shown in Figure 2.[¶] The optical band gap energies were estimated from the extrapolation of the linear parts of corresponding curves to $F(R_d) = 0$.

The Kubelka–Munk function is $F(R_d) = (1 - R_d)^2/(2R_d)$, where R_d is the absolute reflectance of the sample layer.¹³

Compound **1** has an optical band gap E_g of 2.88 eV, however the optical band gap of **2** (1.59 eV) is closer to that of MAPbI_3 (Figure 3). The shape of curves changed with the partial replacement of Br by I in compound **1** (samples **2a–e** correspond to Br/I ratios of 1:4, 2:3, 3:2, 4:1 and 9:1 in the systems before reaction, respectively), which indicates the absence of intermediate compounds in the system; thus, the samples of **2a–e** are the mixtures of **1** and **2**. The absorbance spectrum of **2** has peaks at 637, 521 and 442 nm. The peak at 637 nm can be attributed to an

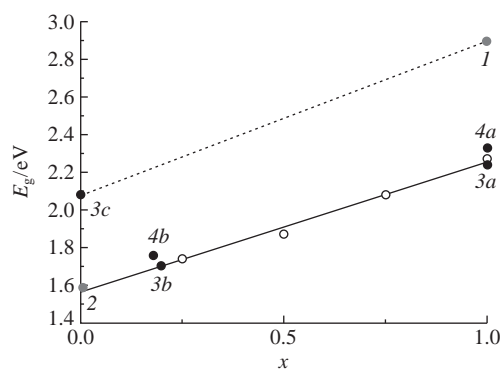


Figure 3 Energy band gaps obtained from the reflectance measurements as a function of Br fractions in (1) **1**, (2) **2**, (3) $\text{PyC}_3\text{BiBr}_5\text{I}_5(1-x)$ ¹¹ or (4) $\text{PyC}_4\text{BiBr}_5\text{I}_5(1-x)$ ¹¹ (a) $x = 1$, (b) $x = 0.18$ – 0.20 , (c) $x = 0$. The hollow circles and a solid line correspond to $\text{MAPbBr}_3\text{I}_3(1-x)$ ⁴.

[¶] The reflectance spectra were measured with a Cary 5000 spectrophotometer in a range of 200–1000 nm at room temperature. PL measurements were performed with a LS55 (Perkin–Elmer) spectrometer in a range of 200–800 nm at room temperature with a resolution of 0.5 nm; the slit width was varied from 10 to 12 nm. Solid-state luminescence measurements were performed using a special module.

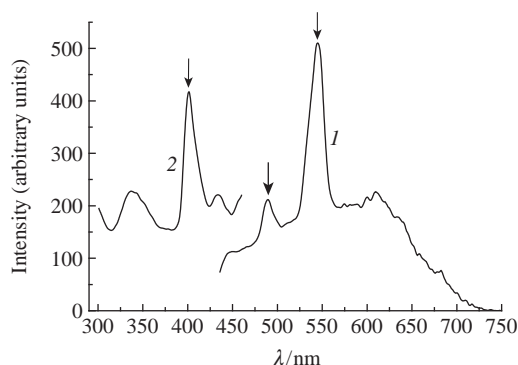


Figure 4 (1) Emission ($\lambda_{\text{ex}} = 401$ nm) and (2) excitation ($\lambda_{\text{em}} = 545$ nm) spectra of **1**.

exciton band with $E_g = 1.59$ eV. The peak at 521 nm can be attributed to a charge transfer band (from BiI_5^{2-} to PyC_5^{2+} or from I to Bi).

The photoluminescence (PL) spectra of crystalline **1** are shown in Figure 4.† The emission spectrum shows two intense PL emission bands at 489 and 545 nm together with a broad band extending over the entire visible region. The most intense emission bands are observed in a long-wave region, and they shifted by ~ 0.60 eV to a low-energy region as compared with optical band gaps. The positions of emission bands indicate that, unlike the lead containing perovskite MAPbI_3 ,¹⁴ this material has an indirect band gap. We suppose that the resulting material has a great number of defects causing the PL enhancement or showing a large exciton binding energy, which had been already observed for organic-inorganic hybrid materials.

Thus, the features of obtained bis(4-cyano-1-pyridino)pentane halobismuthates are similar to those of bis(4-cyano-1-pyridino)propane and bis(4-cyano-1-pyridino)butane halobismuthates. However, $(\text{PyC}_5)_2\text{Bi}_2\text{Br}_{10}$ with a 0-D anion structure is stable, and it does not transform to a semiconductor with 1-D anion chains like $\text{PyC}_3\text{BiBr}_5 \cdot \text{H}_2\text{O}$. The interaction between $(\text{PyC}_5)_2\text{Bi}_2\text{Br}_{10}$ and KI leads to the complete replacement of Br by I and the formation of bis(4-cyano-1-pyridino)pentane iodobismuthate with an optical band gap of 1.59 eV unprecedented for bismuth-containing organic-inorganic hybrid materials, while no exciton bands were observed in the spectra of bis(4-cyano-1-pyridino)propane and bis(4-cyano-1-pyridino)butane iodobismuthates.

The XRD data were collected at the Centre for Collective Use of N. S. Kurnakov Institute of General and Inorganic Chemistry. The NMR data were collected at the NMR Center of A. N. Frumkin

Institute of Physical Chemistry and Electrochemistry. This work was supported by the Ministry of Education and Science of the Russian Federation (project ID: RFMEFI60716X0148).

Online Supplementary Materials

Supplementary data associated with this article can be found in the online version at doi: 10.1016/j.mencom.2017.05.018.

References

- 1 J.-H. Im, J. Luo, M. Franckevičius, N. Pellet, P. Gao, T. Moehl, S. M. Zakeeruddin, M. K. Nazeeruddin, M. Grätzel and N.-G. Park, *Nano Lett.*, 2015, **15**, 2120.
- 2 A. V. Akkuratov, D. K. Susarova, O. A. Mukhacheva and P. A. Troshin, *Mendeleev Commun.*, 2016, **26**, 248.
- 3 A. V. Dmitriev, A. R. Yusupov, R. A. Irgashev, N. A. Kazin, E. I. Mal'tsev, D. A. Lypenko, G. L. Rusinov, A. V. Vannikov and V. N. Charushin, *Mendeleev Commun.*, 2016, **26**, 516.
- 4 B. Suarez, V. Gonzalez-Pedro, T. S. Ripolles, R. S. Sanchez, L. Otero and I. Mora-Sero, *J. Phys. Chem. Lett.*, 2014, **5**, 1628.
- 5 N. Leblanc, N. Mercier, M. Allain, O. Toma, P. Auban-Senzier and C. Pasquier, *J. Solid State Chem.*, 2012, **195**, 140.
- 6 N. A. Yelovik, A. V. Mironov, M. A. Bykov, A. N. Kuznetsov, A. V. Grigorieva, Z. Wei, E. V. Dikarev and A. V. Shevelkov, *Inorg Chem.*, 2016, **55**, 4132.
- 7 D. M. Fabian and S. Ardo, *J. Mater. Chem. A*, 2016, **4**, 6837.
- 8 A. H. Slavney, T. Hu, A. M. Lindenberg and H. I. Karunadasa, *J. Am. Chem. Soc.*, 2016, **138**, 2138.
- 9 R. L. Z. Hoye, R. E. Brandt, A. Osherov, V. Stevanovi, S. D. Stranks, M. W. B. Wilson, H. Kim, A. J. Akey, J. D. Perkins, R. C. Kurchin, J. R. Poindexter, E. N. Wang, M. G. Bawendi, V. Bulović and T. Buonassisi, *Chem. Eur. J.*, 2016, **22**, 2605.
- 10 B.-W. Park, B. Philippe, X. Zhang, H. Rensmo, G. Boschloo and E. M. J. Johansson, *Adv. Mater.*, 2015, **27**, 6806.
- 11 V. Yu. Kotov, A. B. Ilyukhin, K. P. Birin, V. K. Laurinavichyute, A. A. Sadovnikov, Z. V. Dobrokhotova and S. A. Kozyukhin, *New J. Chem.*, 2016, **40**, 10041.
- 12 M. N. Zhidkova, K. E. Aysina, V. Yu. Kotov, V. K. Ivanov, Yu. V. Nelyubina, I. V. Ananyev and V. K. Laurinavichyute, *Electrochim. Acta*, 2016, **219**, 673.
- 13 P. Kubelka and F. Munk, *Z. Tech. Phys.*, 1931, **12**, 593.
- 14 J. Even, L. Pedesseau, J.-M. Jancu and C. Katan, *J. Phys. Chem. Lett.*, 2013, **4**, 2999.
- 15 G. M. Sheldrick, *Acta Crystallogr.*, 2015, **C71**, 3.
- 16 G. M. Sheldrick, *CELL_NOW, Version 2008/4*, Georg-August-Universität Göttingen, Germany, 2008.
- 17 A. A. Coelho, *TOPAS, Version 4.2*, Coelho Software, Brisbane, Australia, 2009.

Received: 10th November 2016; Com. 16/5094